Available online at www.sciencedirect.com
ScienceDirect
International Journal of Mechanical Sciences 49 (2007) 1095–1103
International Journal of MECHANICAL SCIENCES
www.elsevier.com/locate/ijmecsci

Tension transmission via an elastic rod gripped by two circular-edged plates

Jae Ho Jung[a], Ning Pan[a,*], Tae Jin Kang[b]

[a]Department of Biological System Engineering, Division of Textile and Clothing, University of California, Davis, CA 95616, USA
[b]School of Materials Science and Engineering, Seoul National University, Seoul 151-742, South Korea

Received 14 July 2006; received in revised form 28 February 2007; accepted 7 March 2007
Available online 14 March 2007

Abstract

The equilibrium of static friction in tension transmission by an inextensible elastic rod gripped by two plates with round edges was modeled and solved analytically. To proceed, we established equilibrium equations in the deflected and circular edged regions, respectively, and then combined the results together. In both deflected and circular edged region, the condition of cantilever beam with clamped end maintaining a continuous contact was assumed to avoid corresponding mathematical complexity. As a result, we expressed the gripping force in terms of the contact angle, the inclined angle of load, the radius ratio and the initial tension in our results.

More specifically, a more precise but still analytical relationship between the incoming and outgoing tensions including the effect of the rod bending rigidity was derived through the analysis of the circular edged region; it turned out that the radius ratio is the only parameter representing the bending rigidity in the tension ratio. To analyze the deflected region, the classical elastica analysis in terms of an elliptic integral was adopted. Based on the results, the effect of radius ratio and frictional coefficient on the derived force ratio was investigated. As a result, the bending rigidity can be ignored above the range of $\rho \approx 100$. But the tension transmission decreases by 29.1% relative to the classical case at the range of $\rho \approx 5$. In addition, the effect of inclined load on the derived gripping force was also investigated.
© 2007 Published by Elsevier Ltd.

Keywords: Static elastica equilibrium; Transmitted tension; Radius ratio; Continuous frictional contact; Cantilever beam; Capstan equation

1. Introduction

A tensioned rod or film in contact with a circular shaped body is frequently seen in many mechanical set ups and applications. A well-known relationship is the capstan equation [1]. It is very useful for analyzing the process in company with the contact, since the frictional forces are the basis of what holds the equilibrium. However, this equation is not applicable to non-flexible materials because of the involvement of bending moment. Stuart [2] modified the capstan equation, and more thoroughly Jung et al. [3] revised it by including the bending rigidity and radius effect. Another well-known situation is a tensioned rod or film gripped with pressure by the two circular edged plates. This situation can easily be found in textile, film, fiber and yarn processes. Pilled fiber from the fabric undergoes a similar process, and the pull out behavior also shows such a phenomenon, widely known as the shear lag problem.

While we frequently encounter such problems of the tension transmission in many mechanical processes, as is often the case, its approach has been done in rough or approximate way, especially in fibrous and textile area. Although more thorough study was made at Ref. [3], their approach left something to be desired because they used some critical assumptions in applying the force equilibrium to find the incoming and outgoing tension. Therefore, more accurate and rigorous approach should be made through this work.

2. Mathematical modeling

Fig. 1 shows an elastic rod gripped with pressure P and frictional coefficient μ' by two plates of unit thickness whose curvature at the edge is a constant value of $1/r_2$. The rod is pulled out with tension force T_1 at certain angle ϕ of

*Corresponding author.
E-mail address: npan@ucdavis.edu (N. Pan).

0020-7403/$ - see front matter © 2007 Published by Elsevier Ltd.
doi:10.1016/j.ijmecsci.2007.03.003

Nomenclature

P	gripping force
T	tension force
Q	shear force
N	normal force
F_μ	frictional force
M	bending moment
EI	bending rigidity of the rod
μ	static frictional coefficient between rod and circular shaped body at contact region
μ'	static frictional coefficient between rod and plate at gripped region
r_1	radius of the rod
r_2	radius of the circular shaped body
R	total radius, $r_1 + r_2$
s	arc length from the tip end
ϖ	slope angle at arbitrary position of non-contact region
γ	slope angle at pulled tip
ρ	radius ratio between rod and body, r_2/r_1
ω	actual inclined angle of pull-out tension T_1
ϕ	apparent inclined angle of pull-out tension T_1
φ	contact angle from the start point to arbitrary point
θ	total contact angle

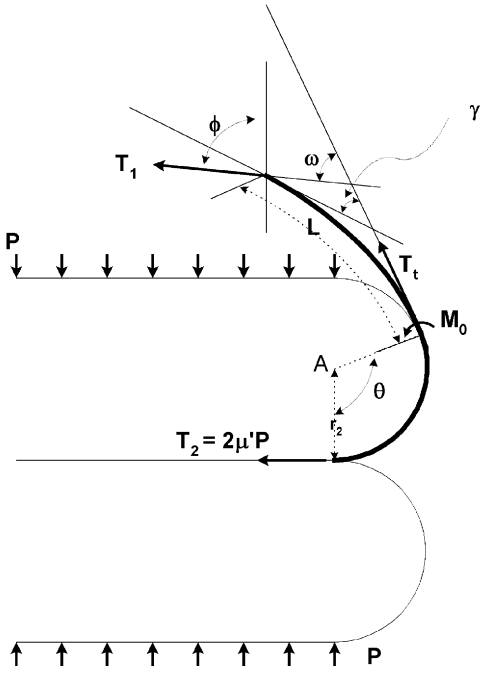

Fig. 1. An elastic rod gripped with pressure P by the two plates whose curvature at the edge is a constant value of $1/r_2$.

inclination measured from the fixed vertical line. Once the rod comes out from the gripped region, it contacts closely with the circular edge over a contact angle θ, beyond which the contact ceases and the rod deflects as if it were a cantilever beam in the boundary condition of one-end-clamp. Due to existence of frictional forces at both the gripped and contact regions, the rod is at a static equilibrium. For convenience of analysis, all existent contacts are regarded as continuous. The possibility of discrete contacts can be avoided by assuming that the contact angle θ is smaller than 180°, or that the tension remains positive so that the inclined angle γ of tension is smaller than 90°. Therefore, we confine the range of ω as $0<\omega<\pi/2$. The range of γ lies in $0<\omega<\pi$ (see Ref. [2]). We also assume that the rod is a linear elastic inextensible material for convenience. To proceed with the analysis, one must consider the equilibrium at both the deflected and circular edged regions.

2.1. Equilibrium at deflected region

Fig. 2 shows a schematic diagram of the equilibrium shape of the rod at the deflected region. In this region, the rod is treated as a cantilever beam in with one-end-clamped. First, the equilibrium equations at point O are as follows:

$$M_1 = T_1 X \sin\omega - T_1 Y \cos\omega, \tag{1}$$

$$\begin{aligned} M(s) &= M_1 + T_1 y\cos\omega - T_1 x \sin\omega \\ &= T_1(X-x)\sin\omega - T_1(Y-y)\cos\omega, \end{aligned} \tag{2}$$

$$M(s) = EI\left(-\frac{\mathrm{d}\varpi}{\mathrm{d}s}\right), \quad \frac{\mathrm{d}M}{\mathrm{d}s} = -EI\left(\frac{\mathrm{d}^2\varpi}{\mathrm{d}s^2}\right), \tag{3}$$

$$\frac{\mathrm{d}^2\varpi}{\mathrm{d}\xi^2} = -\lambda^2 \sin(\omega - \varpi), \tag{4}$$

$$\xi = \frac{s}{L}, \quad \lambda = \frac{T_1 L}{EI}, \tag{5}$$

where M_1 is the bending moment acting at the clamped end, ξ the normalized arc length, and X and Y are the horizontal and vertical deflections relative to the clamped end, respectively. Normalized boundary conditions are the following:

$$\varpi = \gamma, \quad \frac{\mathrm{d}\varpi}{\mathrm{d}\xi} = 0 \quad \text{when } \xi = 0 \text{ at the free end,} \tag{6a}$$

$$\varpi = 0 \quad \text{when } \xi = 1 \text{ at the clamped end.} \tag{6b}$$

Integrating Eq. (4) and determining the integral constant with the boundary condition yields the following:

$$\mathrm{d}\xi = \frac{-\mathrm{d}\psi}{\lambda\sqrt{1 - k^2\sin^2\psi}}, \tag{7}$$

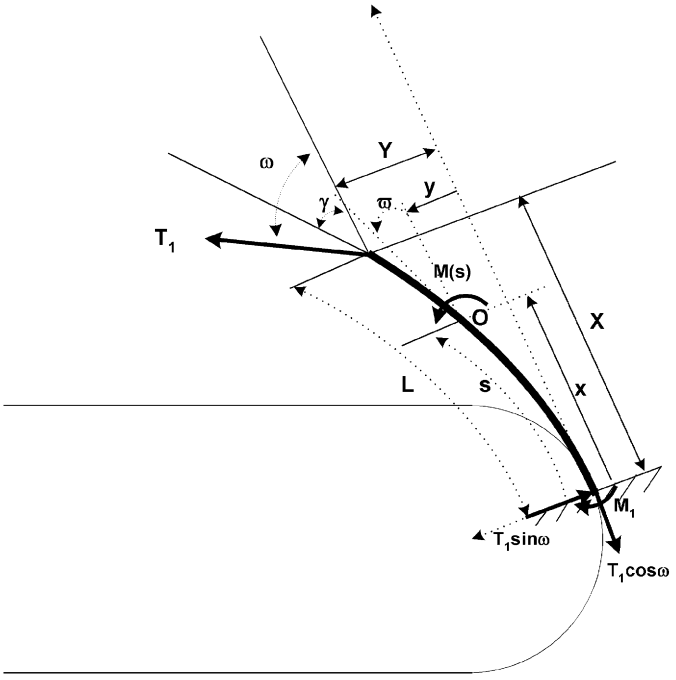

Fig. 2. Schematic diagram of the equilibrium shape of the rod at the deflected region.

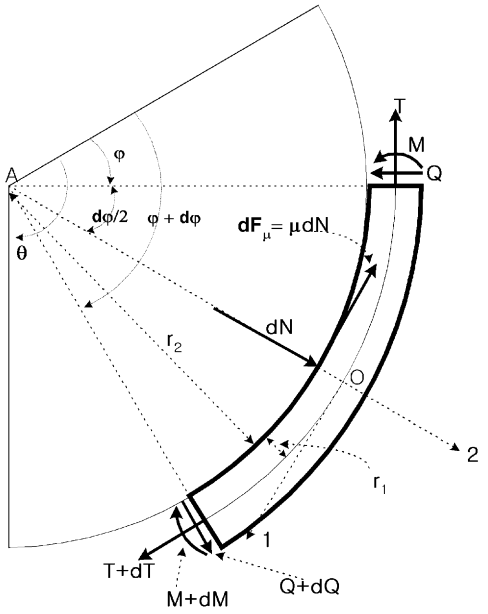

Fig. 3. Exaggerated free body diagram of a rod in contact with a circular edged body.

where ξ is an intermediate parameter and k, ψ are defined as below:

$$k = \sin\frac{\pi-\omega+\gamma}{2} = \cos\left(\frac{\omega-\gamma}{2}\right),$$
$$k\sin\psi = \sin\frac{\pi-\omega+\varpi}{2} = \cos\left(\frac{\omega-\varpi}{2}\right). \quad (8)$$

The transformed boundary conditions are the following:

$$\xi = 0, \quad \varpi = \gamma, \quad \psi = \frac{\pi}{2}, \quad (9a)$$

$$\xi = 1, \quad \varpi = 0, \quad \psi = \psi_c, \quad \psi_c = \arcsin\left\{\frac{\cos(\omega/2)}{\cos((\omega-\gamma)/2)}\right\}. \quad (9b)$$

Integrating Eq. (7) and calculating the tip coordinates X and Y gives

$$\lambda = \sqrt{\frac{T_1L^2}{EI}} = F\left(k,\frac{\pi}{2}\right) - F(k,\psi_c), \quad (10)$$

$$X = \sqrt{\frac{EI}{T_1}}\Big[2\cos\omega\left\{G\left(k,\frac{\pi}{2}\right) - G(k,\psi_c)\right\} - \cos\omega\left\{F\left(k,\frac{\pi}{2}\right) - F(k,\psi_c)\right\} - k\sin\omega\cos\psi_c\Big], \quad (11a)$$

$$Y = \sqrt{\frac{EI}{T_1}}\Big[2\sin\omega\left\{G\left(k,\frac{\pi}{2}\right) - G(k,\psi_c)\right\} - \sin\omega\left\{F\left(k,\frac{\pi}{2}\right) - F(k,\psi_c)\right\} - k\cos\omega\cos\psi_c\Big], \quad (11b)$$

where $F(k,\psi)$ and $G(k,\psi)$ are the standard elliptic integral of first and second kind, respectively. Detailed procedure of derivation will be presented in Appendix A. Substituting the above results into Eq. (1) gives the following equation:

$$M_1 = \sqrt{EI}\cdot\sqrt{T_1}\cdot k\cos\psi_c \quad (12a)$$

$$\text{or, } \frac{M_1}{\sqrt{EI\cdot T_1}} = \cos\left(\frac{\omega-\gamma}{2}\right)\cos\left\{\arcsin\left\{\frac{\cos(\omega/2)}{\cos((\omega-\gamma)/2)}\right\}\right\}. \quad (12b)$$

Eqs. (10)–(12) are the results at the deflected region. They will be used to calculate the transmitted tension T_t and the force ratio P/T_1 in terms of T_1, ω, γ, θ and other parameters together with the results of the next section.

2.2. Equilibrium at the circular edged region

To establish the equilibrium equation at the contact region, we must take into account the force and moment elements acting on the free body diagram in Fig. 3. Considering the force balance along with 1 and 2 directions and the moment balance at point O, we obtain the three equilibrium equations as follows:

$$\sum F_1 = (T+\mathrm{d}T)\cos\frac{\mathrm{d}\varphi}{2} - T\cos\frac{\mathrm{d}\varphi}{2} + (Q+\mathrm{d}Q)\sin\frac{\mathrm{d}\varphi}{2} + Q\sin\frac{\mathrm{d}\varphi}{2} - \mathrm{d}F_\mu = 0, \quad (13)$$

$$\sum F_2 = (Q+\mathrm{d}Q)\cos\frac{\mathrm{d}\varphi}{2} - Q\cos\frac{\mathrm{d}\varphi}{2} - (T+\mathrm{d}T)\sin\frac{\mathrm{d}\varphi}{2} - T\sin\frac{\mathrm{d}\varphi}{2} + \mathrm{d}N = 0, \quad (14)$$

$$\sum M_0 = (M + \mathrm{d}M) - M - (Q + \mathrm{d}Q)\frac{R\mathrm{d}\varphi}{2} - Q\frac{R\mathrm{d}\varphi}{2} + \mathrm{d}F_\mu r_1 = 0, \tag{15}$$

where T, Q, M is the tension, shear force and bending moment, N and F_μ is the normal and frictional force, μ is the frictional coefficient between rod and body in the circular contact region, φ is an angle measured from the start point of contact to an arbitrary point in the contact region, θ the whole contact angle, r_1 and r_2 are the radii of curvature of the rod and the circular edge, respectively, and $R = r_1 + r_2$. In Eq. (15), the origin of Q and T is considered to be on the centerline of the fiber, while the origin of N and F_μ on the contact surface. Taking the limit $\mathrm{d}\varphi \to 0$ and rearranging Eqs. (13)–(15) give the following three differential equations:

$$\mathrm{d}T + Q\,\mathrm{d}\varphi - \mathrm{d}F_\mu = 0, \tag{16}$$

$$\mathrm{d}Q - T\,\mathrm{d}\varphi + \mathrm{d}N = 0, \tag{17}$$

$$\mathrm{d}M - QR\,\mathrm{d}\varphi + r_1\,\mathrm{d}F_\mu = 0, \tag{18}$$

$$\rho = \frac{r_2}{r_1}, \quad R = r_1 + r_2.$$

Bearing in mind that the rod is a linear elastic material and the contact profile is circular, we can derive the following equations:

$$\mu\frac{\mathrm{d}^2T}{\mathrm{d}\varphi^2} + (1+\rho)\frac{\mathrm{d}T}{\mathrm{d}\varphi} - \mu\rho T = 0, \tag{19}$$

$$\frac{\mathrm{d}F_\mu}{\mathrm{d}\varphi} = \frac{1+\rho}{\rho}\frac{\mathrm{d}T}{\mathrm{d}\varphi}, \quad Q = \frac{1}{\rho}\frac{\mathrm{d}T}{\mathrm{d}\varphi}, \quad F = \mu N,$$

$$M = M_0 = \frac{E}{R}\cdot\frac{\pi r_1^4}{4}, \quad \frac{\mathrm{d}M}{\mathrm{d}\varphi} = 0. \tag{20}$$

Eq. (19) together with Eqs. (20) is the governing equation of equilibrium at the contact region. It has the following analytical solution:

$$T(\varphi) = C_1\mathrm{e}^{\alpha\varphi} + C_2\mathrm{e}^{\beta\varphi},$$

$$\alpha = \frac{-1-\rho-\sqrt{(1+\rho)^2+4\mu^2\rho}}{2\mu}, \quad \beta = \frac{-1-\rho+\sqrt{(1+\rho)^2+4\mu^2\rho}}{2\mu}. \tag{21}$$

Applying the above condition to Eqs. (20) and solving them generates the following formulae:

$$Q = \frac{1}{\rho}\frac{\mathrm{d}T}{\mathrm{d}\varphi} = \frac{1}{\rho}(C_1\alpha\mathrm{e}^{\alpha\varphi} + C_2\beta\mathrm{e}^{\beta\varphi}), \tag{22}$$

$$\mathrm{d}N = \frac{1+\rho}{\mu\rho}\frac{\mathrm{d}T}{\mathrm{d}\varphi} = \frac{1+\rho}{\mu\rho}(C_1\alpha\mathrm{e}^{\alpha\varphi} + C_2\beta\mathrm{e}^{\beta\varphi})\,\mathrm{d}\varphi, \tag{23}$$

$$\mathrm{d}F_\mu = \frac{1+\rho}{\rho}(C_1\alpha\mathrm{e}^{\alpha\varphi} + C_2\beta\mathrm{e}^{\beta\varphi})\,\mathrm{d}\varphi. \tag{24}$$

Boundary condition of Eq. (21) is the following:

$$T(0) = C_1 + C_2 = T_1\cos\omega. \tag{25}$$

Yet we cannot determine integral constants C_1 and C_2 from the above equations alone. Therefore, we need one more relationship to determine them. We will find it in next section.

2.3. Expression of transmitted tension and force ratio

To find the relationship between C_1 and C_2, we must consider the total force equilibrium combining the results from both Sections 2.1. and 2.2. Fig. 4 shows a general sketch of the equilibrium state of the rod under the inclined tension and the frictional gripping force. Since the rod comes into contact with the plate at the circular edge, there will exist tension, shear, normal and frictional forces. They will collectively assure a static equilibrium so that the rod may not slide or move.

To establish the force and moment equilibrium, we must calculate the infinitesimal element of force and moment by considering the microscopic element as shown in Fig. 5. Fig. 5 shows all the existing forces and moment acting on the infinitesimal element of the rod. From Fig. 5, the force element according to the h and v direction, and moment element acting on point "A" can be calculated as follows respectively:

$$\begin{aligned}\mathrm{d}(\Sigma F)_h =& -(T+\mathrm{d}T)\sin(\varphi+\mathrm{d}\varphi) + T\sin\varphi - (Q+\mathrm{d}Q)\cos(\varphi+\mathrm{d}\varphi) + Q\cos\varphi \\ &+ \mathrm{d}N\cos\left(\varphi+\frac{\mathrm{d}\varphi}{2}\right) + \mathrm{d}F_\mu\sin\left(\varphi+\frac{\mathrm{d}\varphi}{2}\right) \\ =& -\sin\varphi\mathrm{d}T - T\cos\varphi\mathrm{d}\varphi - \cos\varphi\mathrm{d}Q + Q\sin\varphi\mathrm{d}\varphi + \cos\varphi\mathrm{d}N + \sin\varphi\mathrm{d}F_\mu,\end{aligned} \tag{26}$$

$$\begin{aligned}\mathrm{d}(\Sigma F)_v =& (T+\mathrm{d}T)\cos(\varphi+\mathrm{d}\varphi) - T\cos\varphi - (Q+\mathrm{d}Q)\sin(\varphi+\mathrm{d}\varphi) + Q\sin\varphi \\ &+ \mathrm{d}N\sin\left(\varphi+\frac{\mathrm{d}\varphi}{2}\right) - \mathrm{d}F_\mu\cos\left(\varphi+\frac{\mathrm{d}\varphi}{2}\right) \\ =& \cos\varphi\mathrm{d}T - T\sin\varphi\mathrm{d}\varphi - \sin\varphi\mathrm{d}Q - Q\cos\varphi\mathrm{d}\varphi + \sin\varphi\mathrm{d}N - \cos\varphi\mathrm{d}F_\mu,\end{aligned} \tag{27}$$

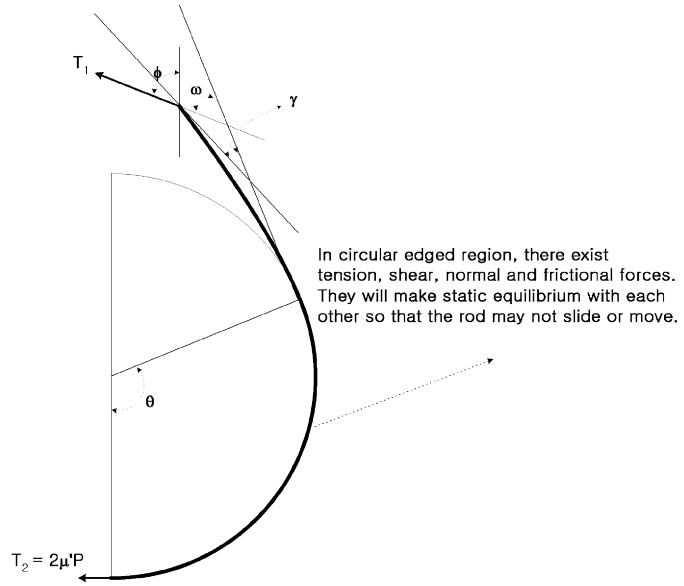

Fig. 4. Macroscopic view of the equilibrium shape of a rod under the inclined tension and the frictional gripping force.

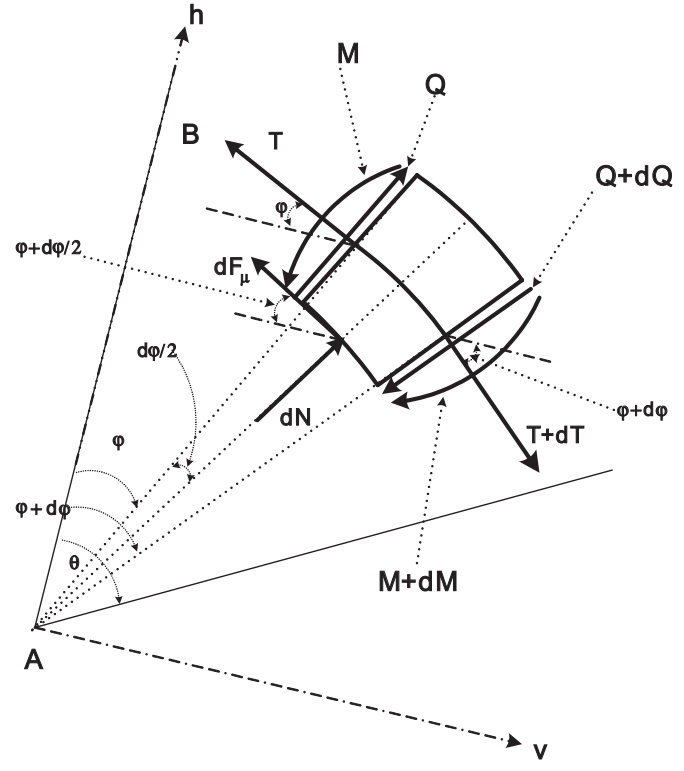

Fig. 5. Microscopic view of the equilibrium condition of force elements existing at the circular edged region and its boundary.

$$\mathrm{d}(\Sigma M)_A = (T+\mathrm{d}T)R - TR + M + \mathrm{d}M - M - r_2\,\mathrm{d}F_\mu = R\,\mathrm{d}T + \mathrm{d}M - r_2\,\mathrm{d}F_\mu = 0$$

$$\left(\text{since } \mathrm{d}T = \frac{r_2}{R}\mathrm{d}F_\mu, \quad \mathrm{d}M = 0\right). \tag{28}$$

Eq. 28 implies that the moment acting at point "A" is always zero, which leads to indeterminate solution. Meanwhile, the total summation of the force element according to the h direction should be zero by static equilibrium of whole contact region. Or

$$\begin{aligned}(\Sigma F)_h &= \int_0^\theta \mathrm{d}(\Sigma F)_h \\ &= -\int_0^\theta \sin\varphi\,\mathrm{d}T - \int_0^\theta T\cos\varphi\,\mathrm{d}\varphi \\ &\quad -\int_0^\theta \cos\varphi\,\mathrm{d}Q + \int_0^\theta Q\sin\varphi\,\mathrm{d}\varphi \\ &\quad +\int_0^\theta \cos\varphi\,\mathrm{d}N + \int_0^\theta \sin\varphi\,\mathrm{d}F_\mu = 0.\end{aligned} \tag{29}$$

Substituting Eqs. (21)–(24) into Eq. (29) and rearranging it gives the following:

$$\begin{aligned}&C_1A_\alpha(\theta) + C_2A_\beta(\theta) = 0,\\ &A_k(\theta) = f_k(\theta)\left\{-k + \frac{k}{\rho} + \frac{(1+\rho)k}{\rho}\right\} \\ &\quad + g_k(\theta)\left\{-1 - \frac{k^2}{\rho} + \frac{(1+\rho)k}{\mu\rho}\right\},\\ &f_k(\theta) = \int_0^\theta \mathrm{e}^{k\varphi}\sin\varphi\,\mathrm{d}\varphi \\ &\quad = \frac{k\mathrm{e}^{k\theta}\sin\theta + (1-\mathrm{e}^{k\theta}\cos\theta)}{k^2+1},\\ &g_k(\theta) = \int_0^\theta \mathrm{e}^{k\varphi}\cos\varphi\,\mathrm{d}\varphi \\ &\quad = \frac{\mathrm{e}^{k\theta}\sin\theta - k(1-\mathrm{e}^{k\theta}\cos\theta)}{k^2+1}.\end{aligned} \tag{30}$$

Combining the above equation with Eq. (25) gives the following:

$$\begin{aligned}C_1 &= \frac{A_\beta(\theta)}{A_\beta(\theta) - A_\alpha(\theta)}T_1\cos\omega,\\ C_2 &= -\frac{A_\alpha(\theta)}{A_\beta(\theta) - A_\alpha(\theta)}T_1\cos\omega.\end{aligned} \tag{31}$$

Substituting Eq. (31) into (21) and putting $\varphi = \theta$ yield the result below.

$$\frac{T(\theta)}{T(0)} = \frac{A_\beta(\theta)\,\mathrm{e}^{\alpha\theta} - A_\alpha(\theta)\,\mathrm{e}^{\beta\theta}}{A_\beta(\theta) - A_\alpha(\theta)}. \tag{32}$$

Eq. (32) is the modified capstan equation with rod rigidity. Note that it is independent of the configuration of deflected region. So the usage of Eq. (32) is not confined to our specific case; it should provide correction to existing approaches in dealing with such problems.

It should also be noted that when including the bending rigidity EI of the rod, the modulus of the rod E itself does not appear in the tension ratio. Instead, the ratio of the radii takes the place. In other words, the tensile modulus of the rod E only influences the value of $T(0)$ and the equilibrium configuration in the deflected region. Whereas the radius ratio here acts as the parameter reflecting the rigidity effect. Bearing in mind that $T(0) = T_1\cos\omega$ and

$T(\theta) = T_2 = 2\mu' P$, we can obtain the following equations:

$$\frac{P}{T_t} = \frac{P}{T_1 \cos\omega} = \frac{1}{2\mu'} \cdot \frac{A_\beta(\theta)\, e^{\alpha\theta} - A_\alpha(\theta)\, e^{\beta\theta}}{A_\beta(\theta) - A_\alpha(\theta)}. \tag{33}$$

Eq. (33) is the ratio between input tension and gripping force. Similarly, it is the individual value of T_1 that is affected by the bending rigidity of the rod, not the force ratio P/T_1. Combining the above equation with (12) gives

$$\frac{PR^2}{EI}\left[\cos\left(\frac{1-\kappa}{2}\omega\right) \cdot \cos\left\{\arcsin\left\{\frac{\cos(\omega/2)}{\cos(((1-\kappa)/2)\omega)}\right\}\right\}\right]^2 = \frac{\cos\omega}{2\mu'} \cdot \frac{A_\beta(\theta)\, e^{\alpha\theta} - A_\alpha(\theta)\, e^{\beta\theta}}{A_\beta(\theta) - A_\alpha(\theta)}, \tag{34}$$

where κ is the ratio between inclined angle and tip slope angle, or $\kappa = \gamma/\omega$ $(0<\kappa<1)$. From Fig. 1 or 4, the variable ω is expressed in terms of θ and ϕ as

$$\omega = \phi - \theta + \frac{\pi}{2} (0 \leqslant \theta \leqslant \pi). \tag{35}$$

Substituting the above equation into Eq. (34) gives the following:

$$\frac{PR^2}{EI} = \frac{\cos(\phi - \theta + \pi/2)\{A_\beta(\theta)\, e^{\alpha\theta} - A_\alpha(\theta)\, e^{\beta\theta}\}}{2\mu'\left[\cos(((1-\kappa)/2)(\phi - \theta + \pi/2)) \cdot \cos\left\{\arcsin\left\{\frac{\cos(1/2)((\pi/2) + \phi - \theta)}{\cos(((1-\kappa)/2)((\pi/2) + \phi - \theta))}\right\}\right\}\right]^2 \cdot \{A_\beta(\theta) - A_\alpha(\theta)\}}, \tag{36}$$

where

$$A_k(\theta) = f_k(\theta)\left\{-k + \frac{k}{\rho} + \frac{(1+\rho)k}{\rho}\right\} + g_k(\theta)\left\{-1 - \frac{k^2}{\rho} + \frac{(1+\rho)k}{\mu\rho}\right\} \quad (k = \alpha, \beta),$$

$$f_k(\theta) = \frac{k e^{k\theta} \sin\theta + (1 - e^{k\theta}\cos\theta)}{k^2 + 1},$$

$$g_k(\theta) = \frac{e^{k\theta}\sin\theta - k(1 - e^{k\theta}\cos\theta)}{k^2 + 1},$$

$$\alpha = \frac{-1 - \rho - \sqrt{(1+\rho)^2 + 4\mu^2\rho}}{2\mu},$$

$$\beta = \frac{-1 - \rho + \sqrt{(1+\rho)^2 + 4\mu^2\rho}}{2\mu},$$

$$R = r_1 + r_2, \quad \rho = r_2/r_1,$$

$$\kappa = \frac{\gamma}{\omega} = \frac{\gamma}{\phi - \theta + \pi/2} \quad (0 \leqslant \theta \leqslant \pi, 0 < \kappa < 1).$$

Eq. (36) is the mathematical manipulation of gripping force in terms of seven parameters—$\phi, \theta, \gamma, EI, \rho, \mu$ and μ'. From the above result, we only need two loading conditions (ϕ, γ) to calculate the gripping force with given geometry—ρ, θ and material properties—EI, μ and μ'. Since it is the final relationship between gripping force and given parameters, it is enough for our goal.

However, we encounter an important question: What is the difference between our result and well-known capstan equation? If on the other hand we use the classical capstan equation to find the ratio between gripping force and transmitted tension, the result can easily be derived as below:

$$\frac{P}{T_t} = \frac{P}{T_1 \cos\omega} = \frac{1}{2\mu'}\, e^{\mu\theta}. \tag{37}$$

Unfortunately the above equation is physically impossible when the bending rigidity of the rod exists. Note that Eq. (33) is more generalized one in the existence of bending rigidity. It also reflects on the effect of radius ratio. If we want more rigorous approach, no doubt we should choose Eq. (33). However, the results are not simple compared with classical capstan equation, nor the obtained result is the same as previous results [1–3]. Therefore we need to compare our result with the classical capstan equation, in that we can figure out how much the error level by choosing classical capstan equation, instead of our results. In order to do so, it is more convenient to choose Eq. (33) than choosing Eq. (36). The effect of inclined angle, radius ratio and frictional coefficient on the difference between classical capstan equation and our result will be presented in Results and Discussions.

3. Results and discussion

It is clear that the inclined angle ω is not included in the right side of Eqs. (33) and (36). So it does not affect the difference between the force ratios calculated by (33) and (37). We are to compare the tendencies of force ratio versus contact angle with each other under the following two different conditions in Cases 1 and 2, which is selected to investigate the influence of the frictional coefficient, and radius ratio on the graph of force ratio versus contact angle at given ratio of $\gamma/\omega = 0.5$. During our calculations, the range of contact angle θ is chosen as $30^\circ \leqslant \theta \leqslant 150^\circ$; the frictional coefficient in the gripped region μ' is assumed the same as in the circular contact region $\mu = \mu'$. To avoid potential discontinued contact problem, the range of ω and γ is confined within the range of $0 < \gamma < \omega < \pi/2$.

Case 1 (μ variation): The values of μ, r_2, ω and γ are chosen as follows:

$$\mu = 0.2, 0.6, \quad \omega = 40^\circ, \quad r_2 = 100 r_1. \tag{37a}$$

Case 2 (r_2/r_1 variation): The values of μ, r_2, ω and γ are chosen as follows:

$$\mu = 0.4, \quad r_2/r_1 = 5, 10, 50, 100, \quad \omega = 40^\circ. \tag{37b}$$

3.1. Results under Case 1—effect of frictional coefficient μ

Figs. 6a and b show the force ratio versus given total contact angle for Case 1. Although it is clear that the classic capstan theory always overestimates the results due to ignoring the bending effect; the error level is not so large than expected under given radius ratio of $\rho = 100$. The maximum error was calculated as 3.95% for $\mu = 0.6$, $\theta = 150^\circ$. So the difference between our result and classical capstan equation is negligible.

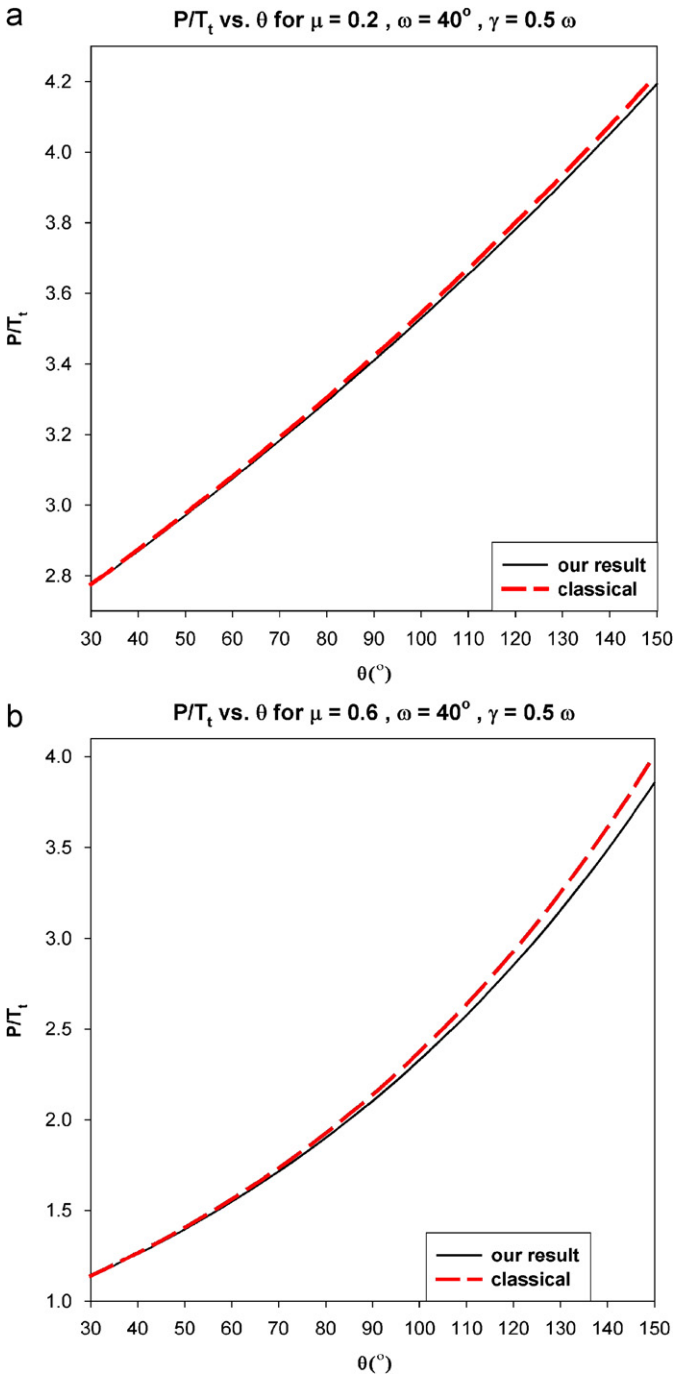

Fig. 6. Comparisons of force ratio of P/T_t versus θ with classical capstan equation at given parameters of $r_2 = 100r_1$, $\omega = 40^\circ$ and $\gamma = 0.5\omega$ for different choice of (a) $\mu = 0.2$, (b) $\mu = 0.6$.

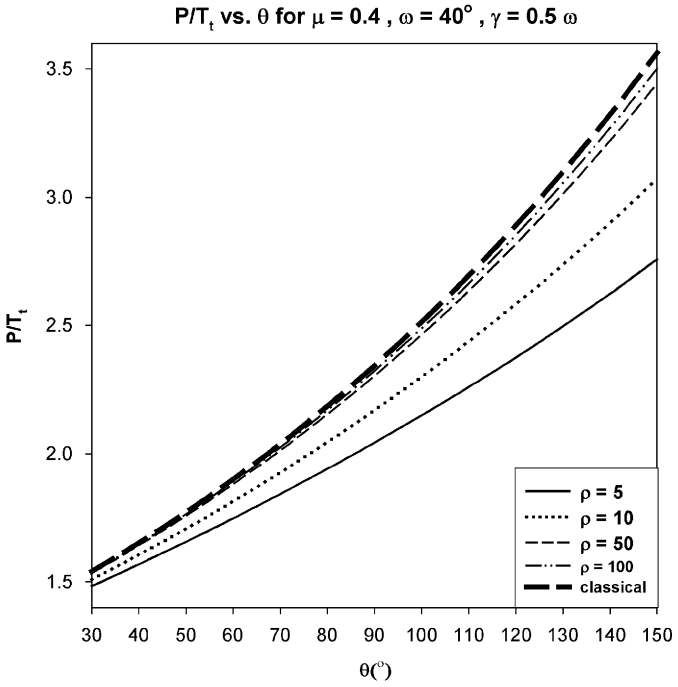

Fig. 7. Comparison of force ratio of P/T_t versus θ for $\mu = 0.4$, $\omega = 40^\circ$, $\gamma = 0.5\omega$ with different choices of $\rho = 5$, 10, 50, 100 with classical capstan equation.

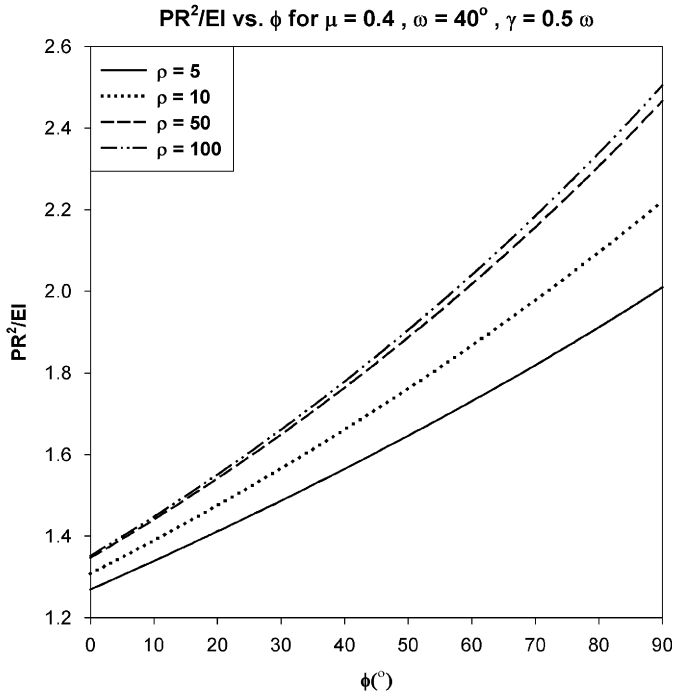

Fig. 8. Normalized gripping force versus ϕ for $\mu = 0.4$, $\omega = 40^\circ$, $\gamma = 0.5$ with different choices of $\rho = 5, 10, 50, 100$ with classical capstan equation.

3.2. Results under Case 2—effect of radius ratio

Fig. 7 shows the force ratio versus the contact angle for Case 2. Also the classical capstan equation overestimates the force ratio due to neglecting the bending rigidity of the rod. However, unlike the Case 1, the error level is sensitive to the radius ratio and cannot be negligible at low level of radius ratio. The error level itself grows smaller as the radius ratio grows larger. Over the range of $\rho = 100$, there is no actual difference between our results and classical one. But the error level is up to 29.1% for the radius ratio of $\rho = 5$. That is, a thinner rod or a thicker pressing plate leads to a smaller error. It is natural tendency since the bending rigidity is directly involved in the radius of the rod. Second moment of area I is the function of the radius of the rod. If the radius of the rod increases, the bending rigidity of the rod also increases, whereas the radius ratio decreases. In fact, the classical capstan equation is the special case of $r_1 = 0$. But more important tendency is that the error depends on the radius ratio, not the radius of the rod itself. It implies that we can diminish the error without changing the properties of the rod by choosing the contact body with larger radius of curvature.

3.3. Effect of inclined angle of load from fixed axis ϕ on the gripping force

From Eq. (36), the gripping force is directly involved with the inclined angle of load(ϕ) from fixed axis. So we are to calculate the normalized gripping force PR^2/EI at given value of $\omega = 40^\circ$, $\gamma = 0.5\omega$:

$$\mu = 0.4, \quad \rho = 5, 10, 50, 100, \quad 0^\circ \leqslant \phi \leqslant 90^\circ. \tag{37c}$$

Fig. 8 shows the graph of normalized gripping force versus ϕ for $\mu = 0.4$, $\omega = 40^\circ$, $\gamma = 0.5$ with different choices of $\rho = 5, 10, 50, 100$. Since the value of ω and γ is fixed, the inserted tension T_1 is constant. The above graph shows the reasonable tendency that the more inclined angle is exerted, the more gripping force is required for the rod not to be on slip. Meanwhile, increasing radius ratio leads to the increase of the required gripping force. Increasing the radius ratio is equal to decrease the bending rigidity. So the required gripping force grows larger.

4. Concluding remarks

We established the mathematical model for explaining the tension transmission of an elastic rod gripped by two circular-edged plates by combining the analysis of contact and non-contact region. In contact, we derived new fundamental differential equations explaining the contact between the rod and body, which leads to the generalized capstan equation with bending rigidity. In non-contact region, we used well-known elastica analysis. By combining two results, we obtained the expression for gripping tension in terms of several geometrical, material and loading parameters. As more rigorous approach than previous attempts, the method of finding the relationship between incoming tension and gripping force was shown in detail, which leads to the exact manipulation of the capstan equation with rigidity. Parametric study carried out in Results and Discussion showed that the classical capstan equation could be acceptable as reasonable approximation in most case, while it is not correct at low level of radius ratio. The most important parameter affecting the difference between our result and the classical one turned out to be the radius ratio.

Acknowledgements

This work was supported by the Korea Research Foundation Grant funded by the Korean Government (MOEHRD, KRF-2005-214-D000407), and National Textile Center (NTC) in University of California at Davis.

Appendix A

Integrating the above Eq. (7) gives

$$\lambda \int_0^1 \mathrm{d}\varepsilon = \int_{\psi_c}^{\pi/2} \frac{\mathrm{d}\psi}{\sqrt{1 - k^2 \sin^2 \psi}}. \tag{A.1}$$

The above leads to Eq. (10). The infinitesimal elements $\mathrm{d}x$ and $\mathrm{d}y$ are expressed as

$$\mathrm{d}x = L\,\mathrm{d}\xi \cos\varpi, \quad \mathrm{d}y = L\,\mathrm{d}\xi \sin\varpi. \tag{A.2}$$

Integrating the above gives

$$X = \frac{L}{\lambda}\int_{\psi_c}^{\pi/2} \cos\varpi\,\mathrm{d}\xi = \frac{L}{\lambda}\int_{\psi_c}^{\pi/2} \frac{(1 - 2k^2\sin^2\psi)\cos\omega + k\sin\omega\sin\psi\sqrt{1 - k^2\sin^2\psi}}{\sqrt{1 - k^2\sin^2\psi}}\,\mathrm{d}\psi, \tag{A.3a}$$

$$Y = \frac{L}{\lambda}\int_{\psi_c}^{\pi/2} \sin\varpi\,\mathrm{d}\xi = \frac{L}{\lambda}\int_{\psi_c}^{\pi/2} \frac{-k\cos\omega\sin\psi\sqrt{1 - k^2\sin^2\psi} + (1 - 2k^2\sin^2\psi)\sin\omega}{\lambda\sqrt{1 - k^2\sin^2\psi}}\,\mathrm{d}\psi, \tag{A.3b}$$

where the first definite integral in the above equations was expressed in terms of ψ using *the theorem of the addition in trigonometric functions*. Similarly they lead to Eqs. (11). Substituting the above into Eqs. (11) leads to Eq. (12a).

Finally, substituting Eq. (20) into (12a) leads to Eq. (12b). The standard elliptic integral of first and second kind is defined as

$$F(k,\psi) = \int_0^{\psi} \frac{\mathrm{d}x}{\sqrt{1-k^2\sin^2 x}},$$
$$G(k,\psi) = \int_0^{\psi} \sqrt{1-k^2\sin^2 x}\,\mathrm{d}x. \quad \text{(A.4)}$$

References

[1] Morton WE, Hearle JWS. Physical properties of textile fibres. 2nd ed. London: Heinemann; 1975. p. 611.
[2] Stuart JM. Capstan equation for strings with rigidity. British Journal of Applied Physics 1961;12:559–62.
[3] Jung JH, Kang TJ, Youn JR. Effect of bending rigidity on the Capstan equation. Textile Research Journal 2004;74(12): 1085–96.